International Journal of Greenhouse Gas Control 100 (2020) 103102

Contents lists available at ScienceDirect

International Journal of Greenhouse Gas Control

journal homepage: www.elsevier.com/locate/ijggc

Heat of absorption of CO_2 in aqueous solutions of DEEA and DEEA + MAPA blends—A new approach to measurement methodology

Hanna Kierzkowska-Pawlak*, Katarzyna Sobala

Lodz University of Technology, Faculty of Process and Environmental Engineering, Ul. Wólczańska 213, 90-924, Łódź, Poland

ARTICLE INFO

Keywords:
CO_2 capture
Heat of absorption
Batch calorimetry
Flow work
Amine blends

ABSTRACT

The heat of absorption is an important parameter that affects the CO_2 absorption and stripping performance of amine-based CO_2 capture. The present paper aims at development of the experimental method of determining the heat of absorption using a batch reaction calorimetry. A prospective high-capacity CO_2-capturing solvent based on an aqueous solution of *N,N*-diethylethanolamine (DEEA) blended with small concentrations of 3-(methyloamino)propylamine (MAPA) is therefore studied. The differential and integral heat of absorption of CO_2 was measured at 40 °C and 60 °C using single DEEA and amine blends. Experiments show that the heat of absorption in DEEA and DEEA + MAPA blends depends both on loading and temperature, though the temperature dependency is not as high as reported earlier. Increasing the MAPA/DEEA concentration ratio increased the heat of absorption in the amine blends.

1. Introduction

CO_2 capture by absorption with aqueous alkanolamines is considered the most feasible technology to reduce CO_2 emissions from fossil-fuel-fired power plants. Although several commercial pilot plants of that type are currently operated, the large energy demand for the solvent regeneration and therefore, high operating costs, are still the major barriers for the widespread deployment of CO_2 capture technologies (Leung et al., 2014; Wilberforce et al., 2019). The other problems lie in large regulatory and legal barriers that have been identified and discussed recently in the literature (Morgan and McCoy, 2012; Dixon et al., 2015).

Amine-based technologies are based on selective absorption-desorption cycles (Eimer, 2014). In principle, the gas absorption combines the physical dissolution of CO_2 in the liquid and subsequent chemical reactions. Amines reversibly react with CO_2 with different mechanisms that affect the overall reaction rate, absorption capacity, heat of absorption and energy requirement for solvent regeneration (Oexmann and Kather, 2010; Chen and Lai, 2019). For primary and secondary amines, the reaction mechanism involved is carbamate formation. The formation of carbamate significantly increases the CO_2 absorption rate but limits the CO_2 absorption capacity. On the contrary, tertiary amines achieve a high CO_2 capacity by forming bicarbonates due to base-catalyzed hydration of CO_2, but the reaction is relatively slow in comparison with carbamate formation (Kierzkowska-Pawlak and Chacuk, 2012). Accordingly, a stable carbamate always requires higher energy to reverse the chemical reaction and regenerate the solvent than bicarbonate. For all these reasons, blended amine systems are typically considered as potential solvents that can achieve the required absorption properties by combining the advantages of each amine. Examples of such mixtures include a base solvent comprising of a tertiary or a sterically hindered amine blended with a fast-reacting primary/secondary amine (Conway et al., 2015; Muchan et al., 2017; Kierzkowska-Pawlak and Kruszczak, 2017; Bernhardsen and Knuutila, 2019).

The heat of absorption represents the combined heat effect due to the physical dissolution of gas in the liquid and the reaction between CO_2 and amine. Generally, the energy required for the solvent regeneration is provided by the reboiler, and is a function of three parameters: (1) heat of CO_2 absorption (ΔH_{abs}), (2) sensible heat to raise the temperature of the solution to the conditions in the reboiler and (3) heat of vaporization of water to generate stripping steam in the regenerator (Oexmann and Kather, 2010; Nwaoha et al., 2017a). Therefore, detailed knowledge of the heat released during the process of CO_2 absorption is necessary to evaluate the performance of the whole installation of CO_2 separation. Moreover, accurate modeling of the absorption column and also predicting the temperature profile, requires the availability of reliable thermodynamic data, including the heat of absorption.

The heat of absorption can be calculated indirectly from the CO_2 solubility data using the Gibbs-Helmholtz equation as following:

* Corresponding author.
E-mail address: hanna.kierzkowska-pawlak@p.lodz.pl (H. Kierzkowska-Pawlak).

https://doi.org/10.1016/j.ijggc.2020.103102
Received 1 April 2020; Received in revised form 1 June 2020; Accepted 18 June 2020

$$\frac{\Delta H_{abs}}{R} = \left(\frac{d(lnp_{CO_2})}{d(1/T)}\right)_{\alpha} \quad (1)$$

where p_{CO2} denotes the partial pressure of CO_2, R is the universal gas constant, T is the temperature and α is the CO_2 loading (mol_{CO2}/mol_{amine}). The application of Eq. (1) is widely discussed in the literature and it is reported that the uncertainty in the determination of the heat of absorption from Eq. (1) is about one order of magnitude higher than the uncertainty in the solubility data (Mathonat et al., 1998; Kim and Svendsen, 2007; Mathias and O'Connell, 2012). Therefore, direct calorimetric measurements always give more accurate values of the heat of absorption than those evaluated by the Gibbs-Helmholtz equation (Nwaoha et al., 2017b). Two typical methods to measure the heat of absorption, including batch calorimetry ("static mode") and flow calorimetry ("dynamic mode"), are used for this purpose. The heat released by introducing a certain amount of gas into the solvent is measured by batch calorimetry using different commercially available reaction calorimeters (Kim and Svendsen, 2007; Liu et al., 2012; Svensson et al., 2013; Mukherjee and Samanta, 2019). Such devices enable time-resolved measurement of the heat flow rate developed during the process. The heat released, by feeding simultaneously a gas component and a solvent at different flow rates to achieve the desired gas loading, is measured by flow calorimetry (Mathonat et al., 1998; Rayer and Henni, 2014).

The present work focuses on the heat effects during CO_2 absorption in aqueous *N,N*-diethylethanolamine (DEEA) solutions and a mixed solvent consisting of two amines: tertiary *N,N*-diethylethanolamine (DEEA) and N-methyl-1,3-propane-diamine (MAPA), which has a primary amine functional group and a secondary one. Recently, the use of the DEEA + MAPA blend has been reported to reveal the superior kinetic performance while maintaining the favorable characteristics of a tertiary DEEA, including a high CO_2 capacity (Garcia and Knuutila, 2017). Our previous studies additionally demonstrated that polyamine MAPA, added even in small concentrations, acts as a very efficient kinetic activator in DEEA solutions (Kruszczak and Kierzkowska-Pawlak, 2017; Kierzkowska-Pawlak and Kruszczak, 2017). However, experimental data with regards to the associated heat of absorption is insufficient (Sobala and Kierzkowska-Pawlak, 2019). In particular, no work has been carried out on the temperature dependence of the heat of absorption in DEEA + MAPA blends containing small concentrations of MAPA. Additionally, with regards to single DEEA solutions, there is no consistency in the literature on the effect of DEEA concentration on the heat of absorption (Kim, 2009; Xu et al., 2014). Therefore, the present research was undertaken to deeper examine the absorption characteristics of these promising absorbents by accurate measuring the heat of CO_2 absorption. Direct calorimetric measurements of the heat of absorption would be very helpful in evaluating the performance of the CO_2 capture process, especially in determining the energy demand for the regeneration of the solvent (Liang et al., 2016). Detailed knowledge of the impact of acid gas loading (mol_{CO2}/mol_{amine}) on the heat of absorption will enable accurate predictions of the temperature profile and rich amine temperature at the exit of the absorption column, providing useful information for the design of CO_2 capture process (Blanchon le Bouhelec et al., 2007).

Measurements are performed for different compositions of DEEA and DEEA + MAPA blends, at various temperatures and CO_2 loadings up to the saturation of the solvent. This research provides deeper insight into the energy balance of the CO_2 absorption process carried out in a batch reaction calorimeter. As a consequence of the involved procedure on the thermal effects resulting from gas dosing to the reactor, a new approach to data interpretation is proposed. We therefore developed the original methodology for batch calorimetric experiments to more accurately subtract the "true" heat effects related to the heat of CO_2 absorption from several apparent heat effects that are associated with the measurement procedure. Our previous data (Sobala and Kierzkowska-Pawlak, 2019) on the heat of absorption is reinterpreted and analyzed together with the new results and literature data.

Table 1
The compositions of the amine solutions studied in this work at 40 °C and 60 °C.

Composition	Concentration (M)
MDEA	2.56 (*studied only at 40°C*)
DEEA	1
	1.5
	2
	3
DEEA + MAPA	0.9 + 0.1
	1 + 0.1
	1.8 + 0.2
	1.9 + 0.1
	1.95 + 0.05

2. Experimental

2.1. Materials

The following reagents were used without further purification: DEEA (Alfa Aesar, mass fraction purity > 99 %), and MAPA (Sigma-Aldrich, mass fraction purity > 98 %). Carbon dioxide was purchased from Linde (mole fraction purity ≥ 99.998 %). For the preparation of aqueous amine solutions distilled and deionized water was used. For weighting the required amount of chemicals, an analytical balance with an accuracy of ± 0.01 g was applied. The uncertainty of determining the concentration is about 0.3 % for low concentrations (1 M), while for larger than 2 M it amounts to 0.1 %. For the validation of the experimental setup, the additional experiments with methyldiethanolamine solutions (MDEA, Sigma-Aldrich, mass fraction purity > 99 %) were performed and the measured heat of CO_2 absorption in 2.56 M MDEA (30 wt. %) at 40 °C was compared with the literature data.

The solutions used are presented in Table 1. The experiments were performed with the single DEEA solutions up to 3 M concentration and the mixtures of DEEA + MAPA up to a total concentration of 2 M, at temperatures of 40 °C and 60 °C. The experimental temperatures match the conditions encountered in the industrial practice. As opposed to the previous research aimed on measurement of the heat of absorption in DEEA + MAPA blends (Arshad et al., 2013; Xu et al., 2014; Knuutila and Nannestad, 2017), the current content of MAPA in DEEA solutions was very small and hence, such mixtures did not give two liquid phases upon CO_2 absorption.

2.2. Experimental procedure

The experiments were conducted in a fully automated, computer-controlled reaction calorimeter (model: CPA201, ChemiSens, Sweden) which offers a direct and on-line measurement of the heat flow developed by the process under isothermal control. The simplified scheme of the experimental setup is shown in Fig. 1. Its detailed description can be found elsewhere (Glotz et al., 2017; Kruszczak and Kierzkowska-Pawlak, 2017; Sobala and Kierzkowska-Pawlak, 2019). The heart of the system is a stainless steel/glass reactor with a volume of about 250 cm^3. The reactor is equipped with an impeller stirrer connected to a magnetically coupled stirrer shaft. The system provides real-time measurements of the heat flow, with no need to re-calibrate before and after the experiment, with an accuracy better than ± 0.01 W. While in use, the reactor is submerged in the thermostating liquid bath, which keeps temperature close to that of the reactor. The reactor is equipped with an insulating, double walled glass jacket to minimize heat flow through the glass walls. By this design, the only path for heat transport from the reactor to the thermostating liquid is though the bottom base, as indicated by the bold arrows in Fig. 1. It is a unique solution that is used

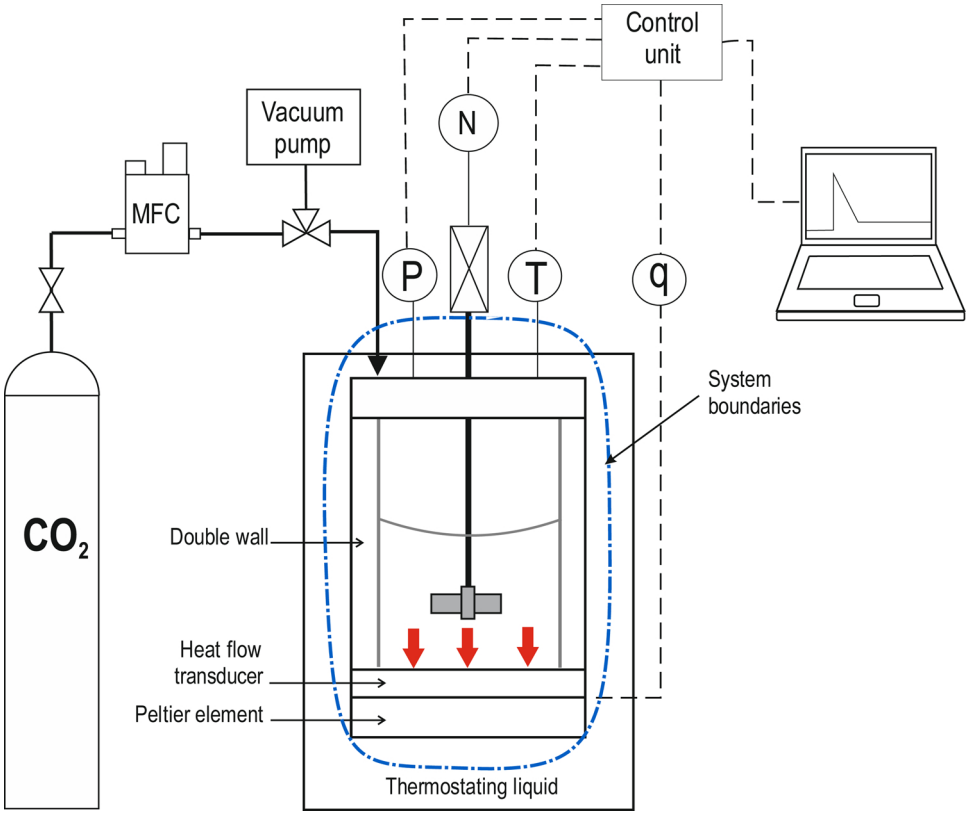

Fig. 1. The apparatus for measuring the heat of absorption of CO_2: MFC – mass flow controller; P - pressure in the reactor; N – stirring speed; T – temperature; q – heat flow. The bold arrows indicate the path for heat exchange with the surrounding liquid.

exclusively by Syrris ChemiSens CPA200 series calorimeters. A major advantage of the CPA201 calorimeter is that the reactor does not require routine calibration since the heat flow output is validated during the manufacturing process which eliminates many shortcomings of the similar calorimetric methods but based on the heat balance for the circulating (thermostating) liquid.

The experiments must be performed under stirring conditions to provide the homogeneity of temperature in the liquid phase, which is necessary for the accuracy of the heat flow measurement. The reactor temperature sensor controls a Peltier element mounted at the bottom which serves as an efficient heating and cooling device, which keeps the reactor temperature controlled within ± 0.01 K.

A high accuracy pressure transducer (OMEGA; accuracy: 0.05 % of the full range of 0–0.35 MPa) was mounted on the reactor flange and served for measuring the absolute pressure in the reactor. The entire system is connected via a control unit to a computer for process control and data acquisition. During the experimental run, the system measures several process parameters including the heat flow rate, the reactor and thermostat temperatures, pressure in the reactor and stirring speed. The signals are registered every 2 s which plays an important role in further data processing. The applied sampling rate is a few times higher than reported by others using a similar calorimeter CPA122 (ChemiSens, Sweden), but of larger scale (Kim, 2009; Arshad et al., 2013; Xu et al., 2014). The entire set-up is leak proof-tested to provide the reliability of mass balance calculations.

The experimental procedure is the same as described previously (Sobala and Kierzkowska-Pawlak, 2019) and will be briefly repeated here. The reactor is loaded with 100.0 ± 0.1 cm^3 of aqueous amine solution at a given temperature of 40 °C or 60 °C and waited until the whole system reached the set temperature. Then, the reactor was carefully degassed to remove inert gases by connection to a vacuum pump and waited for thermal equilibrium meaning that no change in the reactor temperature (± 0.01 K) and heat flow (± 3%) during at least 10 min occurred. We do realize that it is very important to wait a long time, both before the CO_2 injection and after stopping feeding CO_2, to get the correct and stabilized baseline. Otherwise, insufficient time would lead to the overestimated baseline level and the underestimated values of heat of absorption. In the baseline, some minor effects related to the heat dissipated by the stirrer and heat losses that occur simultaneously during CO_2 absorption are included. We are also aware that the properties of the solvent such as viscosity, thermal conductivity, and heat capacity change slightly with loading, and their combined affect is included in the baseline. For that reason, the baseline is calculated after each dosing step, and considered in the calculation of the heat evolved in the particular loading interval.

Before starting the feeding of CO_2 gas, the pressure in the reactor is noted and the registered solvent vapor pressure (p_{vap}) is assumed constant during the entire dosing sequence of CO_2. In our experiments, CO_2 was transported from a non-thermostated flask thought a non-thermostated feeding line, so it was assumed that its inlet temperature was equal to a constant ambient temperature of T_{amb} = 23 ± 1 °C. Fig. 2 shows the illustration of the experimental procedure for a single dosing step: the reactor pressure, heat flow and mass flow of CO_2 for the experimental run with 2.56 M MDEA at 40 °C are recorded as a function of time.

The CO_2 was fed into the reactor vapor phase via a Bronkhorst mass flow controller working in the range (0–200) mg min^{-1} with an accuracy of 0.1 % of the full scale. The single dosing step took up to 4 min and during that time, the pressure in the reactor increased up to a value denoted as P_o. The introduced amount of CO_2 was in the range of (0.01 – 0.02) mole. It corresponds to a loading span of (0.05 – 0.10) mol_{CO2}/mol_{amine}. The heat generation rate due to exothermic absorption of CO_2 in a liquid at isothermal conditions is continuously registered as a function of time. When the CO_2 flow is stopped by closing the mass flow controller valve, the system is allowed to reach the equilibrium under the stirring conditions, which is confirmed by no change of the final

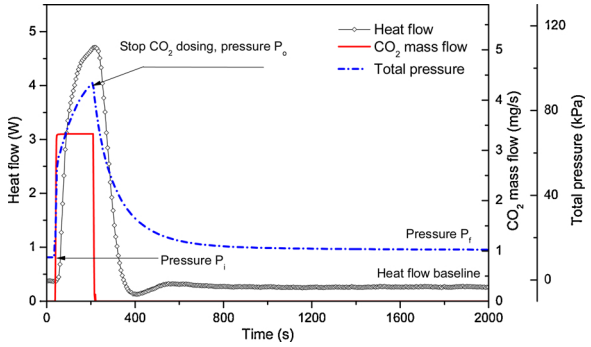

Fig. 2. An example of a heat flow curve, total pressure, and CO_2 mass flow for a single loading interval recorded as a function of time at 2 s intervals (First dosing for the experiment: 2.56 M MDEA, 40 °C). P_i is the total pressure before starting the feeding of CO_2, P_o is the maximum pressure at each dosing step, P_f is the final (equilibrium) pressure at the end of each dosing step.

pressure ($P_f = p_{vap} + p_{CO2} \approx$ const.) and no heat transfer across the bottom of the reactor (heat flow curve reaches the baseline). The above procedure is repeated to gather the heat of absorption data at higher CO_2 loadings.

The recorded signals shown in Fig. 2 indicate that once CO_2 is introduced into the reactor, an increase in total pressure and heat flow can be clearly observed. The temperature in the reactor (not shown on the plot) is only slightly affected by the fast development of heat, due to dosing of CO_2 and subsequent exothermic absorption of CO_2. At about 1500s, the system has reached equilibrium as indicated by the plateau of the heat flow and pressure curves. Then, CO_2 was injected again into the gas phase of the reactor. The procedure of sequential CO_2 dosing was repeated several times. The pressure in the reactor during the entire measurement, including several dosing steps, varied from the solvent vapor pressure p_{vap} before the first injection to about 0.15 MPa during the last loading. Each dosing step lasted between 50–80 min while the whole experiment took 6–14 h to complete. Each experiment consisted of up to 14 equilibrium points. The critical issue in planning the absorption experiments was to reach the saturation of the solvent within a reasonable time. With the increase of amine concentration, the duration of the experiment increases due to the higher absorption capacity and a higher number of dosing steps needed for saturation of the solvent.

Another illustration of the parameters recorded during the whole experiment with CO2 absorption in 2 M DEEA at 60 °C is shown in the Appendix (Fig. A1 in Supplementary material). As can be seen, the heat flow removed by the calorimeter control system to maintain the isothermal conditions has the positive value. However, for the first injection, in the end of the absorption process, the signal of the heat flow drops below the baseline (Fig. 2) or has even a negative value (Fig. A1 in Supplementary material). Such behavior results from the dynamic parameters of the measuring system and is characteristic for the typical response of the proportional–integral–derivative (PID) controller to a rapid heat release. Such a rapid heat release takes place at a high process rate, which occurs at the first dosing step when the solution is "fresh" e.g. not loaded with CO_2.

The separate sets of calibration experiments were performed in order to validate the accuracy of the heat flow signal. The reactor was filled with 100 mL of water at atmospheric pressure, the temperature was set at 40 °C or 60 °C under stirring speed of 400 1/min and an electrical calibration heater was turned on at 4 W for about 5 min. After the calibration heater was turned off, the system was allowed to reach the thermal equilibrium. This validation test was repeated six times for each temperature. The results of these measurements show that the mean relative difference between the amount of heat measured by the calorimetric system and the heat added by the calibration heater, which were both calculated based on the integral of the given heat flow signals, was 1.2 % at 40 °C and 1.3 % at 60 °C. In conclusion, the calibration experiments confirmed the high accuracy of the measuring systems as reported by the producer.

2.3. Analysis of the experiment

To relate the measured signal of the heat flow to the process of interest e.g. solely the absorption of CO_2 in amine solvent, the first law of thermodynamics will be employed. The heat of absorption can be derived from the internal energy balance for the CO_2 absorption carried out in the calorimetric reactor at isothermal conditions (Moran and Shapiro, 2006; Blanchon le Bouhelec et al., 2007). The measuring system can be treated as an unsteady-flow process because the flow rates of mass and energy are not constant across the system boundaries which are indicated in Fig. 2. It is basically an open system since stepwise charging with CO_2 occurs during the absorption process. In this case, external work transfer, namely flow work is transferred into the system through the gas feeding line. In other words, the surrounding has to do work to charge the reactor with additional mass related with dosing of CO_2 (Tosun, 2012; Bhattacharjee, 2019). The flow work is responsible for the additional increase in temperature as the gas fills up the reactor, and therefore it must be subtracted from the total heat effect measured by the calorimeter if we want to estimate the heat of absorption accurately.

The overall heat evolved during the absorption process combined with the associated energy effects of the CO_2 dosing were calculated by integration of the heat flow curve over a particular time interval (Q_{ov}). It should be therefore stressed that this integrated heat measured by the device cannot account solely for the absorption of CO_2 as was usually assumed in studies that follow a similar experimental procedure based on batch calorimetry (e.g. Kim, 2009; Arshad et al., 2013; Xu et al., 2014; Knuutila and Nannestad, 2017). It should be mentioned that all these reported works were conducted on the similar experimental setup (CPA122, ChemiSens, Sweden) and also aimed at measurements of the heat of absorption for MDEA, DEEA and MAPA solutions, and therefore, will be often used as a reference for the discussion of the present methodology.

Therefore, another equation was derived to calculate the heat generated solely by the absorption process denoted here as Q_{abs}:

$$Q_{abs} = Q_{ov} - Q_{sens} + Q_{flow} + (P_f - P_i)V \quad (2)$$

The energy balance expression (2) was formulated based on the first law of thermodynamics adopted for an open system under consideration (Moran and Shapiro, 2006; Blanchon le Bouhelec et al., 2007; Tosun, 2012), distinguishing a few kinds of energy transfer, including heat, enthalpy, and a flow work. The meanings of the particular terms in Eq. (2) are as follows:

- Q_{ov} (J) is the integrated signal of heat flow (W) which is measured and registered by the calorimetric system, Q_{ov} has a negative sign since it denotes the heat removed from the system;
- Q_{sens} (J) is the heat needed to heat the incoming CO2 from the constant ambient temperature (Tamb = 23 ± 1 °C) to the desired temperature (T):

$$Q_{sens} = \Delta n_{CO2} c_v (T - T_{amb}) \quad (3)$$

- Q_{flow} (J) is the flow work term associated with charging the reactor with CO_2 in the amount of Δn_{CO2} and can be estimated from:

$$Q_{flow} = RT\Delta n_{CO2} \quad (4)$$

The last term in eq. (2) represents the enthalpy increase of the system due to the increase of total pressure from the initial pressure P_i to the final pressure P_f (see Fig. 2); V refers to the total volume of the system which is 256 ± 0.1 cm^3 under present experimental conditions. This value affects the heat balance (Eq. 2) and the mass balance of CO_2.

The amount of CO_2 added to the reactor in each dosing step, denoted as Δn_{CO2}, was calculated from the mass flow rate integrated over the dosing time. (Fig. A2). In the present case, this amount of CO_2 (Δn_{CO2}) is being dosed from the temperature of T_{amb} = 23 ± 1 °C which is lower than the process temperature of 40 °C or 60 °C, and a part of heat evolved in the absorption will be therefore consumed for heating the incoming gas stream to the higher temperature.

It should be noted however that the second term in Eq. (2), namely Q_{sens}, was always included in the heat balance in the reported studies by the fact that the CO_2 feed gas was preheated to the same temperature at which the experiment was conducted (Kim, 2009; Arshad et al., 2013; Xu et al., 2014; Knuutila and Nannestad, 2017).

In the literature, two types of the heat of absorption are commonly used: differential heat and integral one. The differential heat of absorption for a certain amine-CO_2 system refers to the heat effect per mole of CO_2 if a very small amount of CO_2 is added into the solution. The integral heat of absorption refers to the heat effect per mole of CO_2 within the CO_2 loading of the solvent increasing from zero to the given loading (Zhang and Chau-Chyun, 2011).

Here, the differential heat of absorption (kJ/mol CO_2) was calculated for each CO_2 dosing from the amount of heat released during the absorption process (Q_{abs}) and the amount of CO_2 absorbed in the liquid (n_{CO_2}):

$$\Delta H_{abs,diff} = \frac{Q_{abs}}{n_{CO_2}} \tag{5}$$

Therefore, the differential heat of absorption is determined for each feeding cycle. The integral heat of absorption is determined by dividing the total amount of heat evolved during the absorption with the total amount of CO_2 absorbed up to the given equilibrium point (Svensson et al., 2014):

$$\Delta H_{abs,int} = \frac{\sum_{i=1}^{n} Q_{abs,i}}{\sum_{i=1}^{n} n_{CO2,i}} \tag{6}$$

The difference between the amount of CO_2 added into the reactor (Δn_{CO2}) and the amount of CO_2 remaining in the gas phase at the physicochemical equilibrium is equal to the amount of CO_2 absorbed (n_{CO_2}). Since the vapor pressure of the solvent (amine + water) was assumed constant during the isothermal absorption, the amount of CO_2 remaining in the gas phase was calculated from the difference between the total final pressure in the reactor (P_f) and the initial pressure (P_i) of each dosing step. The heat of absorption was measured as a function of CO_2 loading which was calculated from:

$$\alpha = \frac{\sum_{i=1}^{n} n_{CO2,i}}{n_{Am}} \tag{7}$$

where: α is the CO_2 loading (mol_{CO2}/mol_{amine}), n_{Am} is the total number of moles of amines in the solution (mol), and "i" denotes the number of a dosing step.

In the present work, dosing the CO_2 through the mass flow controller ensures that the amount of CO_2 transferred to the reactor in each dosing step is calculated with high accuracy. Such a method is unaffected by the rate of absorption which occurs simultaneously during the dosing and also independent of the pressure measurement. Furthermore, knowing the amount of CO_2 transferred to the reactor in each dosing step and the process temperature enables a straightforward calculation of the heat flow work in each dosing step (Eq. 4).

The sources of uncertainty in the present experiments are associated with the amount of CO_2 added into the reactor and subsequently absorbed, as well as the calculated heat released in each CO_2 feeding interval, similarly as identified and described in detail by Kim and Svendsen (2007). The maximum uncertainty in determining the amount of CO_2 added to the reactor and absorbed in the liquid was estimated to be ± 1.4 %. The maximum uncertainty in the integration of the heat flow curve for each CO_2 feeding cycle (Q_{ov}) is determined to be ± 2%, and it results from the manual selection of integration borders and setting the baseline. The uncertainty in determining the amount of heat released during absorption (Q_{abs}) was estimated at ± 2.2 %. Finally, the relative uncertainty in calculating the heat of absorption $\Delta H_{abs,diff}$ was estimated at ± 2.6 % according to:

$$\frac{\sigma \Delta H_{abs,diff}}{\Delta H_{abs,diff}} = \sqrt{\left(\frac{\sigma Q_{abs}}{Q_{abs}}\right)^2 + \left(\frac{\sigma n_{CO_2}}{n_{CO_2}}\right)^2} \tag{8}$$

where σQ_{abs} and σn_{CO2} are the values of uncertainty in the heat released during absorption and the amount of CO_2 absorbed.

3. Results and discussion

3.1. CO_2 + MDEA + H_2O

To check the accuracy of the heat flow measurements in this experimental apparatus and also verify the reliability of the results, initials runs were made for the CO_2 absorption in a single 2.56 M MDEA (methyldiethanolamine) solution at 40 °C and compared with the literature. Since MDEA is a tertiary amine, the reaction of CO_2 with MDEA leads to the formation of bicarbonate ions. The chemical reaction is quite slow and characterized by a low heat of absorption. The heat of CO_2 absorption for this amine has been measured in the past using a similar batch calorimeter (CPA122, ChemiSens, Sweden) and the relevant data is available (Kim, 2009).

Table 2 shows the experimental data and the computed heats of absorption. Data presented in Table 2 allow for assessment of the contribution of individual terms in the heat balance Eq. (2) relative to the measured amount of heat evolved Q_v and the impact of these terms

Table 2
Experimental data on the heat of absorption of CO_2 in 2.56 M MDEA (30 wt %) at 40 °C. Analysis of the contribution of the individual terms in the energy balance according to eq. (2).

α mol_{CO2}/mol_{amine}	$-Q_{ov}$ J	Q_{sens} J	Q_{flow} J	$(P_f-P_i)V$ J	n_{CO2} mol	$-\Delta H_{abs,diff}$ kJ/mol CO_2	$-\Delta H_{abs,diff}$ * kJ/mol CO_2	$-\Delta H_{abs,int}$ kJ/mol CO_2
0.049	725.1	6.1	32.6	0.1	1.25×10^{-2}	55.9	*58.0*	55.9
0.101	738.4	6.3	34.1	0.6	1.30×10^{-2}	54.8	*57.0*	55.3
0.134	481.9	4.1	21.9	0.4	8.34×10^{-3}	55.6	*57.8*	55.6
0.184	716.1	6.2	33.2	0.5	1.26×10^{-2}	54.6	*56.7*	55.0
0.217	458.5	4.0	21.6	0.4	8.20×10^{-3}	53.8	*55.9*	53.8
0.258	563.4	5.0	26.8	0.5	1.02×10^{-2}	53.1	*55.3*	53.4
0.290	451.7	3.9	21.1	0.5	8.01×10^{-3}	54.2	*56.4*	54.2
0.339	703.6	6.1	33.0	0.8	1.25×10^{-2}	54.2	*56.4*	54.2
0.406	952.5	8.3	44.5	1.4	1.67×10^{-2}	54.7	*56.9*	54.7
0.445	553.4	4.8	25.8	1.1	9.66×10^{-3}	55.1	*57.3*	54.8
0.491	661.7	5.8	31.4	1.6	1.17×10^{-2}	54.4	*56.7*	54.4
0.539	679.5	6.0	32.5	2.1	1.20×10^{-2}	54.4	*56.7*	54.4

* $\Delta H_{abs,diff}$ was estimated by neglecting the flow work in the heat balance equation ($Q_{abs} \cong Q_{ov}$).

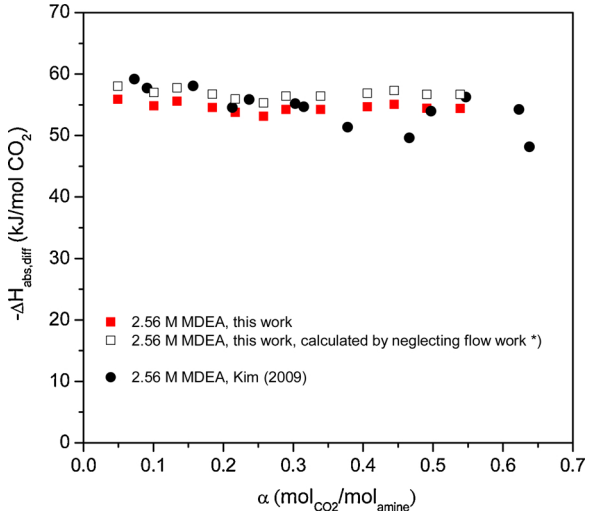

Fig. 3. Differential heat of absorption of CO_2 in 2.56 M MDEA at 40 °C.

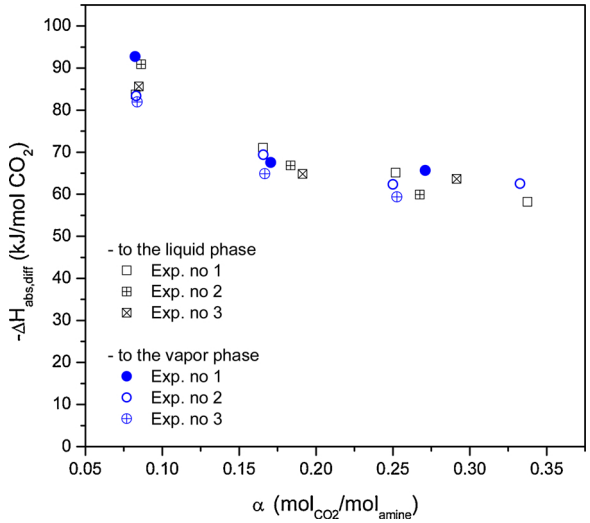

Fig. 4. Heat of absorption of CO_2 in 1 M DEEA at 40 °C measured under different ways of CO_2 dosing: to the vapor phase or the liquid phase.

on the resulting value of heat of absorption. As can be seen, the Q_{sens} heat does not constitute more than 1% of the value of Q_v heat and is within the uncertainty of Q_v determination. Moreover, the contribution of the combined term $(-Q_{sens} + (P_f - P_i)V)$ is even smaller, and therefore, could be safely neglected in the present case. However, the contribution of the flow work accounts from 4.5 to 5 % of the integrated heat flow Q_v, and definitely should not be neglected in the energy balance of the system, as it is typically done by others. Therefore, neglecting the flow work in the analyzed experiments leads to the overestimation of the heat of absorption, denoted as $\Delta H_{abs,diff}$ * in Table 2, by about 5%.

Fig. 3 shows a comparison of the heat of absorption determined in this work, with the data of Kim (2009). At 40 °C, the present differential enthalpy of absorption is close to constant in the range of experimental loading span, $\alpha < 0.55$ (mol_{CO2}/mol_{amine}). Kim (2009) performed measurements in a similar batch calorimeter of a larger scale (2 L) and used a similar methodology. In addition, CO_2 was also injected into the gas phase of the reactor. The heat removed from the reactor by the circulating cooling water was measured in real time and directly applied in the calculation of ΔH_{abs}, without any additional corrections. But it should be emphasized, that the second term in Eq. (2) was however taken care in the heat balance by the fact that the CO_2 feed gas was preheated to the same temperature at which the absorption was conducted.

It can be seen that the present data agree quite well with the data of Kim (2009) and the difference between both data sets is in the range of 2 − 5 kJ/mol CO_2. The data of Kim (2009) is however more scattered, especially for $\alpha > 0.4$ (mol_{CO2}/mol_{amine}) and a bit higher than the present data. On the other hand, if we calculate the differential heat of absorption directly from the measured heat removed by the system (Q_v), as was done by Kim (2009) (e.g. by neglecting the flow work in the energy balance equation), an excellent agreement is obtained between both sets of data in the loading range of 0.05 − 0.4 (mol_{CO2}/mol_{amine}). To summarize, the correct operation and methodology were demonstrated by measuring the heat of absorption of 2.56 M MDEA at 40 °C and comparing it with the literature data. Moreover, we believe that by including the flow work term in the energy balance of the system, the heat of absorption is more accurately determined. As a consequence, the resulting values are smaller than the corresponding ones calculated by neglecting the flow work term ($-\Delta H_{abs,diff} < -\Delta H_{abs,diff}$*, see Table 2).

3.2. CO_2 + DEEA + H_2O

3.2.1. Influence of the method of the CO_2 dosing

As described in the Experimental section, in the present work CO_2 is typically introduced to the vapor phase of the reactor by a port in the lid. This procedure was applied in the experiments with MDEA solutions. However, in the present case, we additionally wanted to ensure whether the method of dosing of CO_2 to the reactor, to the vapor phase or directly to the liquid phase, will affect the results. Therefore, two methods of gas dosing were compared for the absorption of CO_2 into 1 M solution of DEEA at 40 °C while keeping other process parameters the same. Three repetitive measurements were performed for the same experimental conditions by feeding CO_2 through the reactor top and similarly, by feeding CO_2 directly into the liquid phase. All tests were done up to 4 loading intervals. The aim of the described experiments was also to check the reproducibility of measurements.

Fig. 4 shows the results of differential heat of absorption determined by applying different ways of gas dosing. We can observe that only the first data points, obtained for the first loading interval, at $\alpha = 0.06$ (mol_{CO2}/mol_{amine}), are scattered which was also observed by others using a batch calorimetry technique. Generally, two data sets show a similar small dispersion regardless of the method of gas dosing. Moreover, the presented data sets for higher loadings reveal a sufficiently good reproducibility and it seems that the method of CO_2 dosing does not affect the measured amount of heat generated during the process, as shown by our systematic measurements. Although the rate of absorption was a bit higher when CO_2 was dosed directly into the liquid, it had no impact on the individual terms in the energy balance Eq. (2). Therefore, we can safely compare different data sets measured by a batch calorimetry technique, irrespective of the method of CO_2 dosing.

This conclusion is, however, in contradiction with the findings of Kim et al. (2014) who studied the heat of absorption for monoethanolamine (MEA) solutions. No effect from the way of CO_2 feeding was observed when solutions with higher MEA concentrations (30 and 70 wt.% MEA) were used, while for a 10 wt.% MEA at 120 °C, much higher heat of absorption was reported when CO_2 was fed from the top valve to a vapor phase in comparison to the results gathered when CO_2 was fed to the liquid phase. No explanation was given to account for the observed phenomenon.

3.2.2. Results

The heat of absorption of CO_2 for single DEEA solutions was measured for different concentrations: 1 M, 1.5 M, 2 M and 3 M at

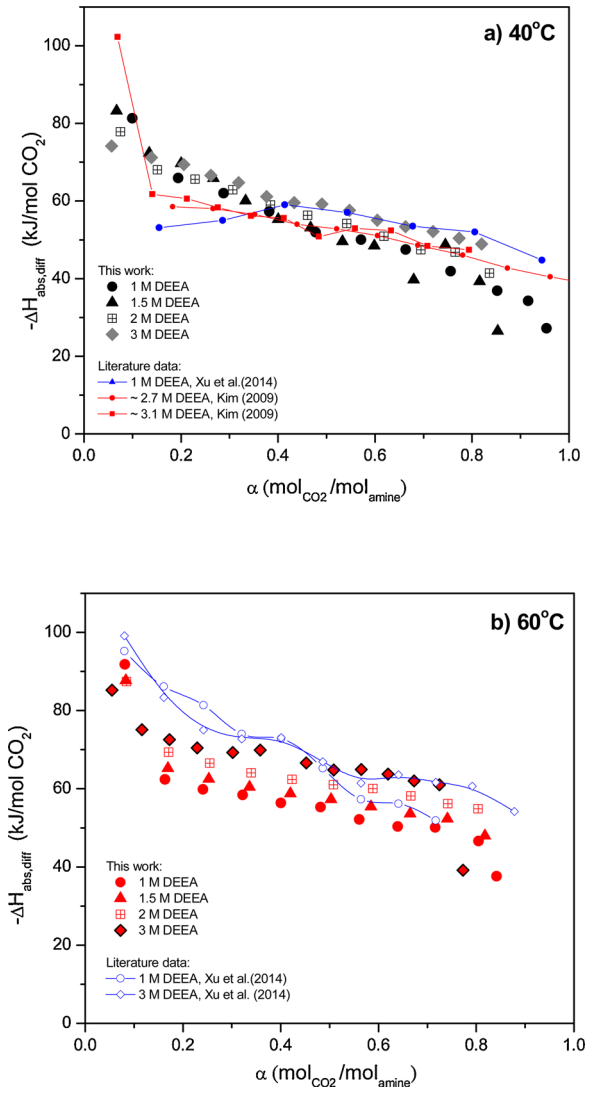

Fig. 5. Differential heat of absorption in single DEEA solutions at 40 and 60 °C. Comparison with literature data. a) 40 °C b) 60 °C.

temperatures of 40 °C and 60 °C, while dosing of CO_2 to the vapor phase. The present results were compared with the limited literature data measured also by a similar batch calorimetry technique while dosing of CO_2 to the vapor phase. Kim (2009) conducted measurements for 2.7 and 3.1 M DEEA, while Xu et al. (2014) for 1, 3, 4 M DEEA and Arshad et al. (2013) for 5 M DEEA solution.

The present results for DEEA solutions were further used as a reference for the assessment of MAPA addition on the heat of absorption in blended amines DEEA + MAPA. The new experimental results in terms of differential and integral heat of absorption in aqueous DEEA are given in Table A1. The experimental data of differential heat of absorption for the different DEEA concentrations as a function of CO_2 loading are also presented graphically in Fig. 5.

The presented data show that the heat of absorption strongly depends on the CO_2 loading of the solution. As can be seen, the heat of CO_2 absorption for each concentration and temperature decreases with increasing CO_2 loading of the solution. Both at 40 °C (Fig. 5a) and 60 °C (Fig. 5b), the differential enthalpy of absorption gradually decreases until loading of approximately 0.8, at which point the $-\Delta H_{abs,diff}$ starts to decrease more steeply. This agrees with the data of Kim (2009); Arshad et al. (2013); Xu et al. (2014). As mentioned earlier, the heat of absorption combines the heat of CO_2 dissolution and the heat of reaction between CO_2 and amine. At CO_2 loadings lower than 0.8, the concentration of molecular CO_2 in the liquid is very low since all the CO_2 which is transferred to the liquid takes part in the chemical reaction with amine leading to the formation of bicarbonate. Thus, the differential heat of absorption is the highest at initial acid gas loadings and generally decreases with increasing CO_2 loading. At loadings approaching 0.8, the fraction of physically absorbed CO_2 increases, and this is revealed by a sharper decrease in the heat of absorption. Although the CO_2 loading effect in the present experimental data is similar as reported previously, the new data give somewhat higher absolute values of heat of absorption at 40 °C and lower absolute values at 60 °C than those measured by others for the similar concentrations (Kim, 2009; Xu et al., 2014).

As discussed in this paper, determining the heat of absorption is affected by several factors, including the heat flow measurement coupled with the energy balance of the calorimetric system and the amount of CO2 absorbed in the solution. It should be emphasized that this data is not measured directly in a batch calorimetric method and is subject to errors, which contribute to the uncertainty of the results. As can be seen, the observed difference between the heat of absorption in DEEA solutions reported here and by others is not significant and may be generally attributed to the mentioned factors. To decide which of these factors affects the observed differences, it would be necessary to analyze the intermediate results of calculations aimed at determining the heat of absolution. In this case, it is not possible, since raw measurement data are not available for the referenced papers (Kim, 2009; Xu et al., 2014).

As discussed by many authors, there is a disagreement in the literature on the relationship between the heat of absorption and the amine concentration in the solution (Kim, 2009; Xu et al., 2014; Rayer and Henni, 2014; Arcis et al., 2012). Our results indicate that there is a very weak dependence of amine concentration on the heat of absorption, which can be observed at CO_2 loadings higher than 0.3. Specifically, at 60 °C, it seems that the heat of absorption increases slightly with DEEA concentration. However, at lower loadings achieved up to 4 initial dosing steps in our case, the heat of absorption data is scattered, and it is difficult to draw conclusive findings.

Some studies have attempted to explain whether the heat of absorption is independent of DEEA concentration in the solution. Kim (2009) obtained no dependence of the heat of CO_2 absorption on the solution concentration, but the analysis was performed for a narrow DEEA concentration range (2.7 and 3.1 M DEEA) at 80 °C. On the contrary, at 40 °C Xu et al. (2014) noted higher absolute values of $\Delta H_{abs,diff}$ for 4 M DEEA than for 1 M DEEA in the whole CO_2 loading range. However, at temperatures higher than 80 °C, the opposite trend was observed.

The effect of temperature is also not evident. An analysis of the results reported in Fig. 5 and Table A1 suggests that between 40 °C and 60 °C and at low CO_2 loadings, the temperature has rather no effect on the heat of absorption for a given DEEA concentration. Again, since the data on the heat of absorption is scattered in this region, it is impossible to conclude on the character of this relationship. However, a weak increase in the heat of absorption with increasing temperature is seen for higher loadings. For example, for 3 M DEEA solution and loading $\alpha = 0.3$ mol_{CO2}/mol_{amine} the heat of absorption at 40 °C and 60 °C K was $\Delta H_{abs,diff}$ = -64 kJ/mol CO_2 and $\Delta H_{abs,diff}$ = -69 kJ/mol CO_2, respectively. The slight increase in the heat of absorption with increasing temperature was noticeable for each DEEA concentration; however, the observed small increase is within the experimental uncertainty in some cases.

3.3. CO_2 + DEEA + MAPA + H_2O

The heat of absorption of CO_2 for DEEA + MAPA blends was measured at temperatures of 40 °C and 60 °C up to total concentrations of 2 M. The new experimental data in terms of differential and integral heat of absorption in DEEA + MAPA blends are given in Tables A2–A6.

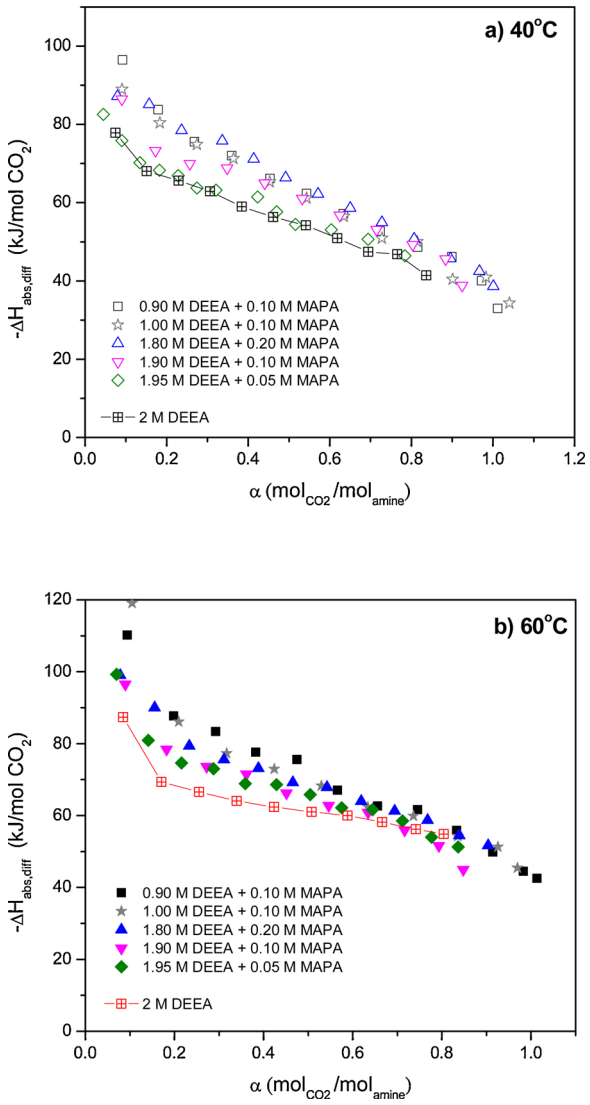

Fig. 6. Differential heat of absorption of CO_2 in DEEA + MAPA blends at 40 °C and 60 °C. Comparison with single 2 M DEEA solution. a) 40 °C b) 60 °C.

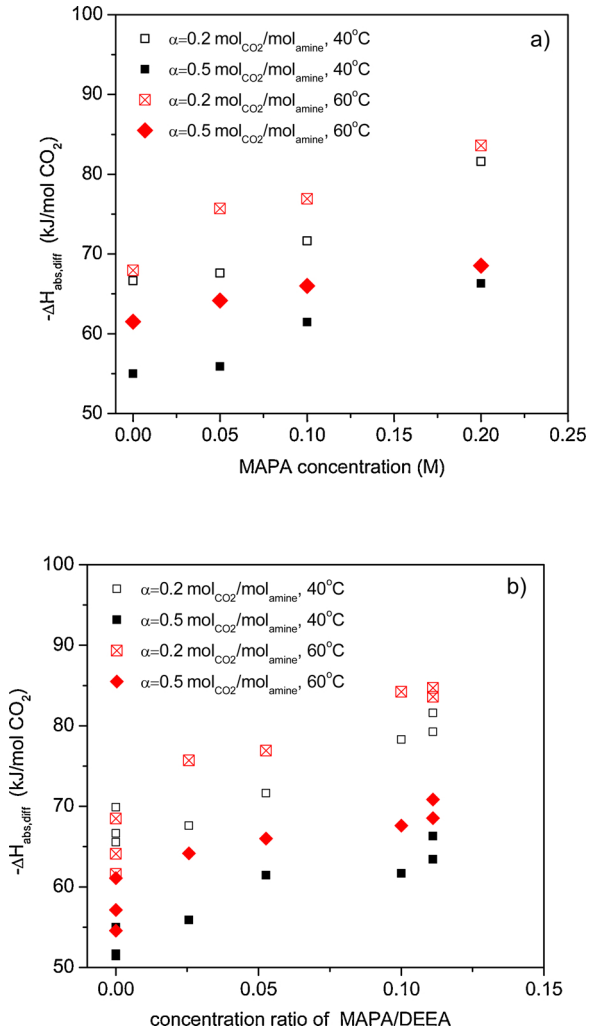

Fig. 7. The impact of solvent compositions on the heat of absorption at different CO_2 loadings at 40 °C and 60 °C. a) The impact of MAPA concentration on the heat of absorption for: 1.95 M DEEA + 0.05 MAPA, 1.9 M DEEA + 0.1 MAPA, 1.8 M DEEA + 0.2 MAPA. b) The impact of MAPA/DEEA ratio on the heat of absorption for: 1-3 M DEEA, 1.95 M DEEA + 0.05 MAPA, 1.9 M DEEA + 0.1 MAPA, 1.8 M DEEA + 0.2 MAPA, 0.9 M DEEA + 0.1 MAPA, 1 M DEEA + 0.1 MAPA.

The results can be further expressed as the heat per mole of amine (kJ/mol amine) by multiplying ΔH_{abs} (kJ/mol CO_2) with the loading.

Differential heat of absorption for the following blends: 0.9 M DEEA + 0.1 M MAPA, 1 M DEEA + 0.1 M MAPA, 1.8 M DEEA + 0.2 M MAPA, 1.9 M DEEA + 0.1 M MAPA, 1.95 M DEEA + 0.05 M MAPA, is also presented graphically in Fig. 6 as a function of CO_2 loading. The relevant data on the heat of absorption obtained for a single 2 M DEEA solution is additionally plotted for comparison.

The heat of absorption in amine blends decreases with the increase in CO_2 loading, as in the case of pure DEEA solutions. Knuutila and Nannestad (2017) and Arshad et al. (2013) reported that for the DEEA + MAPA blends containing 1–5 M MAPA, initially, a very small decline in the heat of absorption occurred with the increase of loading up to $\alpha = 0.5$ mol_{CO2}/mol_{amine}, and then, after exceeding $\alpha = 0.5$ mol_{CO2}/mol_{amine}, a much faster and steeper decrease was observed. In the present case, such a two-stage relationship is not reported since we used much smaller additions of MAPA (0.05, 0.1, 0.2 M MAPA).

The obtained values show that the dependence of $\Delta H_{abs,diff}$ as a function of the CO_2 loading, at both temperatures and all concentrations, follow a similar trend. As can be seen from Fig. 6 (as well as from Fig. 7), the values of heat of absorption obtained for DEEA + MAPA blends at 60 °C are slightly higher than the ones at 40 °C. The analysis of the present data additionally reveals that by varying the concentration of DEEA, from 0.9 to 1.9 M while keeping the same MAPA concentration of 0.1 M, the heat of absorption decreases. In DEEA + MAPA blends, polyamine MAPA reacts first with CO_2, due to its fast reaction rate leading to carbamate formation (Garcia et al., 2017; Bernhardsen and Knuutila, 2019). At low CO_2 loadings, the heat of absorption for 1.8 M DEEA + 0.2 M MAPA blend is close to the value for a single MAPA. The heat of absorption of single 1 M MAPA at 40∘C and loading 0.2 mol_{CO2}/mol_{amine} has been reported to be around 84 kJ/mol (Arshad et al., 2013). Later, as the loading increases, DEEA starts reacting and the heat of absorption reaches values close to single DEEA solutions.

By comparing the heat of absorption for DEEA + MAPA blends and single DEEA solution (2 M) in Fig. 7a, one can see that the addition of MAPA causes a visible increase in the differential heats of CO_2 absorption, which were estimated for two loadings: $\alpha = 0.2$ mol_{CO2}/mol_{amine} and $\alpha = 0.5$ mol_{CO2}/mol_{amine}. The effect is most pronounced for 1.8 M DEEA + 0.2 M MAPA blend, e.g. for the highest content of MAPA, at both temperatures. At 40 °C, however, for very small MAPA additive (0.05 M), the heat of absorption for 1.95 M DEEA + 0.05 M MAPA overlaps the experimental points for pure 2 M DEEA, within the experimental uncertainty.

To better illustrate the influence of relative concentration of MAPA

to DEEA in the solvent, expressed here by MAPA/DEEA ratio, on the heat of absorption, another plot is made in Fig. 7b. It shows the impact of MAPA/DEEA ratio on the heat of absorption for different solutions: 1.95 M DEEA + 0.05 MAPA, 1.9 M DEEA + 0.1 MAPA, 1.8 M DEEA + 0.2 MAPA, 0.9 M DEEA + 0.1 MAPA, 1 M DEEA + 0.1 MAPA, 1 − 3 M DEEA. It is clear that the heat of absorption, estimated at two temperatures for given loadings (0.2 and 0.5), increases with the increasing concentration ratio MAPA/DEEA.

4. Conclusions

In the present work the heat of absorption of CO_2 in aqueous DEEA solutions and DEEA + MAPA blends was measured as a function of CO_2 loading at 40 °C and 60 °C, using a batch calorimetry technique. Because this amine system has been recognized as a promising solvent alternative, the main motivation was to study in detail the effect of small MAPA concentrations on the heat of absorption in DEEA solutions.

The present research provides a deeper understanding of the impact of gas transport to the reactor on the heat balance of the batch calorimetric system and a more rigorous methodology of determination of the heat of absorption in such kind of calorimeters. The present work shows that the contribution of flow work accounts up to 5% of the integrated heat flow, which is directly measured by the device, and definitely should not be neglected in the energy balance of the system. Therefore, the proposed calculations, based on the energy balance Eq. (2) which includes flow work, give more accurate values of the heat of absorption. Since the heat of absorption is directly related to the energy requirement for the solvent regeneration, it is desirable that it should be determined precisely to avoid uneconomic overdesign.

Generally, as the CO_2 loading increases, the heat of CO_2 absorption gradually decreases for all data series, which is in line with the literature findings. Experiments show that at 40 °C the heat of absorption in DEEA solutions seems to be independent of the solution concentration within the experimental uncertainty. However, at 60 °C, increasing the concentration in the range of 1 − 3 M DEEA increased the heat of absorption. The heat of absorption in DEEA solutions slightly increases with temperature, though the temperature dependence is not as significant as was reported earlier.

The present study indicated that the heat of absorption in DEEA + MAPA blends depends both on the temperature and composition of the solvent. Increasing temperature and the MAPA/DEEA concentration ratio increased the heat of absorption.

CRediT authorship contribution statement

Hanna Kierzkowska-Pawlak: Conceptualization, Data curation, Formal analysis, Methodology, Supervision, Writing - review & editing. **Katarzyna Sobala:** Investigation, Data curation, Visualization, Writing - original draft.

Declaration of Competing Interest

The authors declare that they have no known competing financial interests or personal relationships that could have appeared to influence the work reported in this paper.

Appendix A

Table A1
Integral and differential heats of absorption of CO_2 in DEEA solutions as a function of loading.

Loading mol_{CO2}/mol_{amine}	$-\Delta H_{abs,diff}$ kJ/mol CO_2	$-\Delta H_{abs,int}$ kJ/mol CO_2	Loading mol_{CO2}/mol_{amine}	$-\Delta H_{abs,diff}$ kJ/mol CO_2	$-\Delta H_{abs,int}$ kJ/mol CO_2
1 M DEEA					
40 °C			60 °C		
0.099	60.79	60.79	0.081	104.37	104.37
0.194	70.10	65.34	0.164	56.67	80.38
0.288	63.05	64.59	0.241	55.17	72.26
0.382	58.32	63.05	0.322	55.10	67.96
0.478	52.95	61.03	0.400	55.55	65.53
0.571	51.06	59.39	0.481	53.17	63.45
0.664	48.55	57.88	0.561	50.05	61.55
0.756	45.10	56.32	0.640	48.23	59.91
0.852	37.82	54.23	0.716	47.93	58.63
0.916	41.06	53.31	0.805	44.36	57.05
0.954	31.49	52.45	0.841	35.03	56.10
1.5 M DEEA					
40 °C			60 °C		
0.067	86.07	86.07	0.083	87.05	87.05
0.135	75.16	80.60	0.169	62.98	74.83
0.200	72.58	77.96	0.253	60.26	70.00
0.267	68.69	75.65	0.336	58.16	67.07
0.333	62.97	73.14	0.420	56.49	64.95
0.400	58.13	70.62	0.503	55.02	63.31
0.467	55.96	68.51	0.585	53.13	61.89
0.533	52.50	66.54	0.665	51.35	60.62
0.599	51.39	64.88	0.741	49.98	59.53
0.680	38.62	61.75	0.818	45.53	58.21
0.745	55.75	61.22			
2 M DEEA					
40 °C			60 °C		
0.075	77.67	77.67	0.085	82.98	82.98

(*continued on next page*)

Table A1 (*continued*)

Loading mol_{CO2}/mol_{amine}	$-\Delta H_{abs,diff}$ kJ/mol CO_2	$-\Delta H_{abs,int}$ kJ/mol CO_2	Loading mol_{CO2}/mol_{amine}	$-\Delta H_{abs,diff}$ kJ/mol CO_2	$-\Delta H_{abs,int}$ kJ/mol CO_2
0.151	67.82	72.70	0.171	63.25	73.06
0.229	65.42	70.22	0.255	62.13	69.45
0.307	62.98	68.39	0.340	59.64	67.00
0.385	59.07	66.51	0.423	57.95	65.21
0.461	56.43	64.83	0.508	56.59	63.78
0.542	54.28	63.26	0.589	55.49	62.64
0.619	51.03	61.74	0.666	53.55	61.58
0.695	47.57	60.19	0.742	51.46	60.55
0.765	47.03	58.98	0.804	49.51	59.70
0.836	41.77	57.51			
2 M DEEA					
40 °C			60 °C		
0.057	69.51	69.51	0.055	80.76	80.76
0.139	69.24	69.35	0.116	66.55	73.28
0.205	67.28	68.68	0.172	66.40	71.04
0.262	64.30	67.74	0.229	64.89	69.52
0.319	62.45	66.79	0.302	64.97	68.42
0.376	58.84	65.57	0.358	65.51	67.97
0.433	57.29	64.49	0.452	63.47	67.03
0.490	56.89	63.60	0.509	61.00	66.36
0.547	55.33	62.74	0.565	61.10	65.84
0.605	52.74	61.79	0.619	59.84	65.31
0.663	51.12	60.85	0.673	58.08	64.73
0.720	49.82	59.98	0.725	56.99	64.18
0.773	47.99	59.15	0.773	35.02	62.36
0.820	46.32	58.43			

Table A2
Integral and differential heats of absorption of CO_2 in 0.9 M DEEA + 0.1 M MAPA as a function of loading.

Loading mol_{CO2}/mol_{amine} 40 °C	$-\Delta H_{abs,diff}$ kJ/mol CO_2	$-\Delta H_{abs,int}$ kJ/mol CO_2	Loading mol_{CO2}/mol_{amine} 60 °C	$-\Delta H_{abs,diff}$ kJ/mol CO_2	$-\Delta H_{abs,int}$ kJ/mol CO_2
0.092	96.4	96.4	0.094	110.2	110.2
0.179	83.7	90.3	0.198	87.7	98.4
0.268	75.6	85.4	0.293	83.3	93.5
0.360	72.0	82.0	0.383	77.6	89.8
0.454	66.1	78.7	0.475	75.6	87.0
0.543	62.3	76.0	0.566	67.1	83.8
0.634	57.2	73.3	0.656	62.6	80.9
0.724	52.7	70.8	0.746	61.7	78.6
0.816	48.6	68.3	0.833	55.8	76.2
0.899	46.2	66.2	0.914	49.9	73.9
0.972	40.0	64.2	0.983	44.5	71.8
1.012	32.9	63.0	1.014	42.5	70.9

Table A3
Integral and differential heats of absorption of CO_2 in 1 M DEEA + 0.1 M MAPA as a function of loading.

Loading mol_{CO2}/mol_{amine} 40 °C	$-\Delta H_{abs,diff}$ kJ/mol CO_2	$-\Delta H_{abs,int}$ kJ/mol CO_2	Loading $mol_{CO2}/mola_{amine}$ 60 °C	$-\Delta H_{abs,diff}$ kJ/mol CO_2	$-\Delta H_{abs,int}$ kJ/mol CO_2
0.091	89.0	89.0	0.105	119.1	119.1
0.184	80.4	84.7	0.210	86.1	102.6
0.275	74.8	81.4	0.317	77.3	94.0
0.365	71.2	78.9	0.424	72.9	88.7
0.454	65.3	76.2	0.530	68.2	84.6
0.544	61.2	73.7	0.634	62.4	81.0
0.636	56.5	71.3	0.736	59.9	78.0
0.728	50.9	68.7	0.836	54.2	75.2
0.815	50.1	66.7	0.926	51.3	72.9
0.902	40.4	64.2	0.970	45.4	71.6
0.984	40.9	62.2			
1.041	34.4	60.7			

Table A4
Integral and differential heats of absorption of CO_2 in 1.8 M DEEA + 0.2 M MAPA as a function of loading.

Loading mol_{CO2}/mol_{amine} 40 °C	$-\Delta H_{abs,diff}$ kJ/mol CO_2	$-\Delta H_{abs,int}$ kJ/mol CO_2	Loading mol_{CO2}/mol_{amine} 60 °C	$-\Delta H_{abs,diff}$ kJ/mol CO_2	$-\Delta H_{abs,int}$ kJ/mol CO_2
0.079	88.0	88.0	0.078	98.99	98.99
0.157	86.0	87.0	0.155	90.01	94.53
0.237	79.3	84.4	0.233	79.37	89.45
0.336	76.7	82.1	0.311	75.55	85.97
0.414	72.0	80.2	0.388	73.12	83.42
0.492	67.2	78.2	0.466	69.24	81.07
0.572	63.1	76.1	0.543	67.85	79.20
0.650	59.5	74.1	0.619	63.98	77.32
0.728	55.8	72.1	0.694	61.27	75.59
0.807	51.6	70.1	0.768	58.70	73.95
0.896	46.5	67.8	0.839	54.44	72.30
0.967	43.3	66.0	0.904	51.67	70.82
1.001	39.2	65.1			

Table A5
Integral and differential heats of absorption of CO_2 in 1.9 M DEEA + 0.1 M MAPA as a function of loading.

Loading mol_{CO2}/mol_{amine} 40 °C	$-\Delta H_{abs,diff}$ kJ/mol CO_2	$-\Delta H_{abs,int}$ kJ/mol CO_2	Loading mol_{CO2}/mol_{amine} 60 °C	$-\Delta H_{abs,diff}$ kJ/mol CO_2	$-\Delta H_{abs,int}$ kJ/mol CO_2
0.090	86.5	86.5	0.090	96.5	96.5
0.173	73.3	80.2	0.182	78.4	87.3
0.257	70.0	76.9	0.273	73.6	82.8
0.348	68.9	74.8	0.361	71.5	80.0
0.440	65.0	72.7	0.451	66.3	77.3
0.532	61.1	70.7	0.546	62.8	74.8
0.624	56.8	68.7	0.634	60.8	72.8
0.715	53.1	66.7	0.717	55.9	70.9
0.803	49.3	64.8	0.793	51.6	69.0
0.884	45.6	63.0	0.848	45.0	67.5
0.924	38.9	62.0	0.090	96.5	96.5
	86.5	86.5	0.182	78.4	87.3

Table A6
Integral and differential heats of absorption of CO_2 in 1.95 M DEEA + 0.05 M MAPA as a function of loading.

Loading mol_{CO2}/mol_{amine} 40 °C	$-\Delta H_{abs,diff}$ kJ/mol CO_2	$-\Delta H_{abs,int}$ kJ/mol CO_2	Loading mol_{CO2}/mol_{amine} 60 °C	$-\Delta H_{abs,diff}$ kJ/mol CO_2	$-\Delta H_{abs,int}$ kJ/mol CO_2
0.045	83.7	83.7	0.070	99.3	99.3
0.090	77.0	80.3	0.141	81.0	90.0
0.134	71.3	77.4	0.216	74.6	84.7
0.182	69.4	75.3	0.288	73.0	81.8
0.228	68.0	73.8	0.359	68.9	79.2
0.274	64.9	72.3	0.429	68.6	77.5
0.321	64.3	71.2	0.505	65.8	75.7
0.423	62.6	69.1	0.575	62.2	74.1
0.470	58.8	68.1	0.644	61.6	72.7
0.516	55.6	67.0	0.712	58.5	71.4
0.604	54.2	65.1	0.777	54.0	69.9
0.694	51.8	63.4	0.836	51.3	68.6
0.784	47.6	61.5			

Appendix B. Supplementary data

Supplementary material related to this article can be found, in the online version, at doi:https://doi.org/10.1016/j.ijggc.2020.103102.

References

Arcis, H., Ballerat-Busserolles, K., Rodier, L., Coxam, J.Y., 2012. Measurement and modeling of enthalpy of solution of carbon dioxide in aqueous solutions of diethanolamine at temperatures of (322.5 and 372.9) K and pressures up to 3 MPa. J. Chem. Eng. Data 57, 840–855.

Arshad, M.W., Fosbøl, P.L., von Solms, N., Svendsen, H.F., Thomsen, K., 2013. Heat of absorption of CO_2 in phase change solvents: 2-(diethylamino) ethanol and 3-(methylamino) propylamine. J. Chem. Eng. Data 58, 1974–1988.

Bernhardsen, I.M., Knuutila, H.K., 2019. Kinetics of CO_2 absorption into aqueous solutions of 3-dimethylamino-1-propanol and 1-(2-hydroxyethyl) pyrrolidine in the blend with 3-(methylamino) propylamine. Chem. Eng. Sci. X 3, 100032.

Bhattacharjee, S., 2019. TEST: The Expert System for Thermodynamics. Electronic Resource, Entropysoft, San Diego, CA (Accessed 20 December 2019). http://www.thermofluids.net.

Blanchon le Bouhelec, E., Mougin, P., Barreau, A., Solimando, R., 2007. Rigorous modeling of the acid gas heat of absorption in alkanolamine solutions. Energy Fuels 21, 2044–2055.

Chen, P.C., Lai, Y.L., 2019. Optimization in the stripping process of CO_2 gas using mixed amines. Energies 12 (11), 2202.

Conway, W., Bruggink, S., Beyad, Y., Luo, W., Melián-Cabrera, I., Puxty, G., Feron, P., 2015. CO_2 absorption into aqueous amine blended solutions containing monoethanolamine (MEA), N, N-dimethylethanolamine (DMEA), N, N-diethylethanolamine (DEEA) and 2-amino-2-methyl-1-propanol (AMP) for post-combustion capture processes. Chem. Eng. Sci. 126, 446–454.

Dixon, T., McCoy, S.T., Havercroft, I., 2015. Legal and regulatory developments on CCS. Int. J. Greenh. Gas Control 40, 431–448.

Eimer, D., 2014. Gas Treating: Absorption Theory and Practice. John Wiley & Sons.

Garcia, M., Knuutila, H.K., Gu, S., 2017. Determination of kinetics of CO_2 absorption in unloaded and loaded DEEA+ MAPA blend. Energy Procedia 114, 1772–1784.

Glotz, G., Knoechel, D.J., Podmore, P., Gruber-Woelfler, H., Kappe, C.O., 2017. Reaction calorimetry in microreactor environments - measuring heat of reaction by isothermal heat flux calorimetry. Org. Process Res. Dev. 21 (5), 763–770.

Kierzkowska-Pawlak, H., Chacuk, A., 2012. Numerical simulation of CO_2 absorption into aqueous methyldiethanolamine solutions. Korean J. Chem. Eng. 29 (6), 707–715.

Kierzkowska-Pawlak, H., Kruszczak, E., 2017. Revised kinetics of CO_2 absorption in aqueous N, N-diethylethanolamine (DEEA) and its blend with N-methyl-1, 3-propanediamine (MAPA). Int. J. Greenh. Gas Control 57, 134–142.

Kim, I., 2009. Heat of Reaction and VLE of Post Combustion CO_2 Absorbents. Ph.D. Thesis. Norwegian University of Science and Technology, Trondheim, Norway.

Kim, I., Svendsen, H.F., 2007. Heat of absorption of carbon dioxide (CO_2) in monoethanolamine (MEA) and 2-(aminoethyl) ethanolamine (AEEA) solutions. Ind. Eng. Chem. Res. 46 (17), 5803–5809.

Kim, I., Hoff, K.A., Mejdell, T., 2014. Heat of absorption of CO_2 with aqueous solutions of MEA: new experimental data. Energy Procedia 63, 1446–1455.

Knuutila, H.K., Nannestad, Å., 2017. Effect of the concentration of MAPA on the heat of absorption of CO_2 and on the cyclic capacity in DEEA-MAPA blends. Int. J. Greenh. Gas Control 61, 94–103.

Kruszczak, E., Kierzkowska-Pawlak, H., 2017. CO_2 capture by absorption in activated aqueous solutions of N,N-diethylethanolamine. Ecol. Chem. Eng. S 24, 239–248.

Leung, D.Y.C., Caramanna, G., Maroto-Valer, M.M., 2014. An overview of current status of carbon dioxide capture and storage technologies. Renew. Sustain. Energy Rev. 39, 426–443.

Liang, Z., Fu, K., Idem, R., Tontiwachwuthikul, P., 2016. Review on current advances, future challenges and consideration issues for post-combustion CO_2 capture using amine-based absorbents. Chin. J. Chem. Eng. 24, 278–288.

Liu, J., Wang, S., Svendsen, H.F., Idrees, M.U., Kim, I., Chen, C., 2012. Heat of absorption of CO_2 in aqueous ammonia, piperazine solutions and their mixtures. Int. J. Greenh. Gas Control 9, 148–159.

Mathias, P.M., O'Connell, J.P., 2012. The Gibbs–Helmholtz equation and the thermodynamic consistency of chemical absorption data. Ind. Eng. Chem. Res. 51 (13), 5090–5095.

Mathonat, C., Majer, V., Mather, A.E., Grolier, J.P., 1998. Use of flow calorimetry for determining enthalpies of absorption and the solubility of CO_2 in aqueous monoethanolamine solutions. Ind. Eng. Chem. Res. 37 (10), 4136–4141.

Moran, M.J., Shapiro, H.N., 2006. Fundamentals of Engineering Thermodynamics, 5th edition. Wiley, Chichester.

Morgan, M.G., McCoy, S.T., 2012. Carbon Capture and Sequestration: Removing the Legal and Regulatory Barriers, 1st edition. RFF Press, Routledge.

Muchan, P., Saiwan, C., Narku-Tetteh, J., Idem, R., Supap, T., Tontiwachwuthikul, P., 2017. Screening tests of aqueous alkanolamine solutions based on primary, secondary, and tertiary structure for blended aqueous amine solution selection in post combustion CO_2 capture. Chem. Eng. Sci. 170, 574–582.

Mukherjee, S., Samanta, A.N., 2019. Heat of absorption of CO_2 and heat capacity measurements in aqueous solutions of benzylamine, N-(2-aminoethyl)-ethanolamine, and their blends using a reaction calorimeter. J. Chem. Eng. Data 64 (8), 3392–3406.

Nwaoha, C., Idem, R., Supap, T., Saiwan, C., Tontiwachwuthikul, P., Rongwong, W., et al., 2017a. Heat duty, heat of absorption, sensible heat and heat of vaporization of 2–Amino–2–Methyl–1–Propanol (AMP), Piperazine (PZ) and Monoethanolamine (MEA) tri–solvent blend for carbon dioxide (CO_2) capture. Chem. Eng. Sci. 170, 26–35.

Nwaoha, C., Supap, T., Idem, R., Saiwan, C., Tontiwachwuthikul, P., AL-Marri, M.J., Benamor, A., 2017b. Advancement and new perspectives of using formulated reactive amine blends for post-combustion carbon dioxide (CO_2) capture technologies. Petroleum 3 (1), 10–36.

Oexmann, J., Kather, A., 2010. Minimising the regeneration heat duty of post-combustion CO_2 capture by wet chemical absorption: the misguided focus on low heat of absorption solvents. Int. J. Greenh. Gas Control 4, 36–43.

Rayer, A.V., Henni, A., 2014. Heats of absorption of CO_2 in aqueous solutions of tertiary amines: N-methyldiethanolamine, 3-dimethylamino-1-propanol, and 1-dimethylamino-2-propanol. Ind. Eng. Chem. Res. 53 (12), 4953–4965.

Sobala, K., Kierzkowska-Pawlak, H., 2019. Heat of absorption of CO_2 in aqueous N, N-diethylethanolamine+ N-methyl-1, 3-propanediamine solutions at 313 K. Chin. J. Chem. Eng. 27 (3), 628–633.

Svensson, H., Hulteberg, C., Karlsson, H.T., 2013. Heat of absorption of CO_2 in aqueous solutions of N-methyldiethanolamine and piperazine. Int. J. Greenh. Gas Control 17, 89–98.

Tosun, I., 2012. The thermodynamics of phase and reaction equilibria. Newnes.

Xu, Z., Wang, S., Qi, G., Trollebø, A.A., Svendsen, H.F., Chen, C., 2014. Vapor liquid equilibria and heat of absorption of CO_2 in aqueous 2-(diethylamino)-ethanol solutions. Int. J. Greenh. Gas Control 29, 92–103.